PAN AIR Applications to Aero-Propulsion Integration

A. W. Chen* and E. N. Tinoco*
Boeing Commercial Airplane Company, Seattle, Washington

The versatility of the PAN AIR system has led to its application to a variety of aero-propulsion problems. Examples of some of these applications on subsonic transport configurations are presented to illustrate the use of the PAN AIR system. The cases presented include one example in which PAN AIR was coupled to three-dimensional boundary layer analysis for iterative solutions. An internal flow case and several external flow cases are presented. These include a study of the internal flow losses through a calibration nozzle, the calculation of surface pressures about an isolated nacelle, the modeling of exhaust flows, and the analysis of nacelle blowing (power) effects on a complete wing-body-strut-nacelle configuration.

Nomenclature

A = streamtube area
C_D = discharge coefficient
C_L = lift coefficient
C_p = pressure coefficient
C_V = velocity coefficient
c = wing chord
FNPR = fan nozzle pressure ratio
h = vertical distance of fan cowl exit from wing
M = Mach number
$\dot{m}_I$ = ideal mass flow
m_T = transpiration mass flux
$\bar{n}$ = surface unit normal vector
p = static pressure
V = velocity
$\bar{V}$ = total velocity vector
$\bar{W}$ = total mass flux vector
x = streamwise coordinate
y = lateral coordinate
z = vertical coordinate
δ^* = boundary layer displacement thickness
σ = source strength
ρ = air density
θ = boundary layer momentum thickness
Φ = total velocity potential
ϕ = perturbation velocity potential

Subscripts

I = inlet
∞ = freestream

Introduction

THE quest for improved propulsive efficiencies for commercial transport aircraft has led to the development of large diameter high-bypass-ratio turbofan engines. The retrofitting of these large diameter engines to existing aircraft or their integration with new advanced-technology (supercritical) wings can lead to large interference penalties (3 to 5% of aircraft drag) if sufficient care is not taken in the design and development of these installations.[1] Previous nacelle installations based on wind-tunnel methodology have indicated a historical boundary, illustrated in Fig. 1, outside of which minimum nacelle integration drag (1% or less aircraft drag) could be achieved. However, persistent adherence to this boundary in a new design may result in designs with unacceptably low nacelle ground clearance or excessively long landing gear and nacelle strut lengths (excessive weight). Adherence to this boundary could also make retrofit of high-bypass-ratio engines to an existing airframe originally designed for a low-bypass-ratio engine economically impractical. Empirical attempts to develop a low drag nacelle installation inside this boundary have not been too successful. The problems associated with developing a close-coupled high-bypass-ratio engine installation have provided the incentive for a coordinated computational and wind-tunnel development effort begun in the mid 1970's. References 2 and 3 detail some of the early understanding of the nacelle/airframe integration problem. New design procedures, heavily influenced and aided by computational studies, have been instrumental in the retrofitting of new high-bypass-ratio turbofan engines (CFM56) to two existing airframes (B707/KC-135R and B737-300) and in the development of two new aircraft types (B757-200 and B767-200). These new installations, also illustrated in Fig. 1, feature close-coupled nacelle designs well inside the previously defined high drag boundary. Wind-tunnel tests have shown these configurations to exhibit 1% or less nacelle installation drag. Flight-test results (the B737-300 will fly in 1984) also support these low installation drag values. All of the early studies and most of the computational work responsible for these successful designs were based on subcritical panel methods.

In this paper the versatility of a second generation panel method is demonstrated through several examples. PAN AIR[4-7] is a general three-dimensional boundary value problem-solver for the Prandtl-Glauert equation. This panel method, valid for both inviscid linear subsonic and supersonic analyses, has been applied to a variety of aero-propulsion integration problems. In cases where it was desirable to simulate the viscous effects, a boundary layer program was coupled iteratively with PAN AIR in an experimental pilot code. The boundary layer program uses an integral method to calculate three-dimensional turbulent boundary layers.[8] The effect of the boundary layer on the outer inviscid flow is represented through a transpiration boundary condition derived from the boundary layer parameters. The solution is cycled between the inviscid PAN AIR and the boundary layer code until convergence of results from one cycle to the next is achieved. An example of coupled PAN AIR/boundary layer results will be shown.

Currently, PAN AIR exists in pilot code form and in production code form for dissemination throughout the United States. In this paper PAN AIR will refer to the technology embodied in the codes rather than to a specific version of the code.

Recently, finite difference transonic methods have been progressing to the level of geometric complexity and computational accuracy required for certain kinds of

Presented as Paper 83-1368 at the AIAA/SAE/ASME 19th Joint Propulsion Conference, Seattle, Wash., June 27-29, 1983; received July 5, 1983; revision received Oct. 5, 1983.

*Senior Specialist Engineer. Member AIAA.

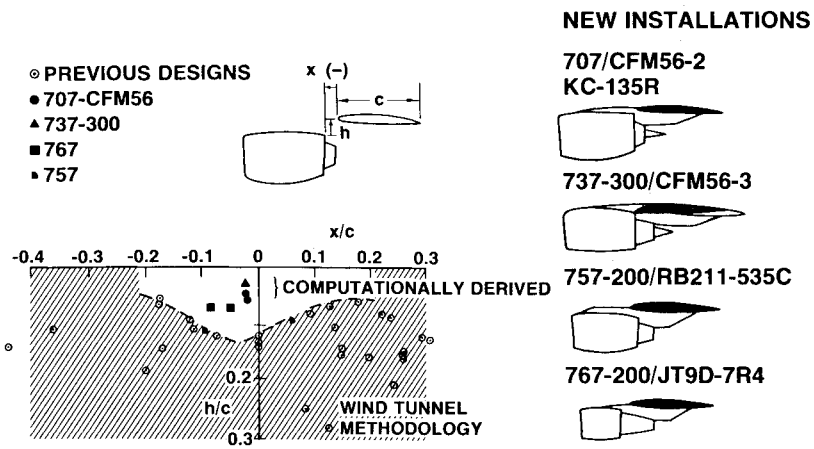

Fig. 1 Computationally derived close-coupled nacelle positions.

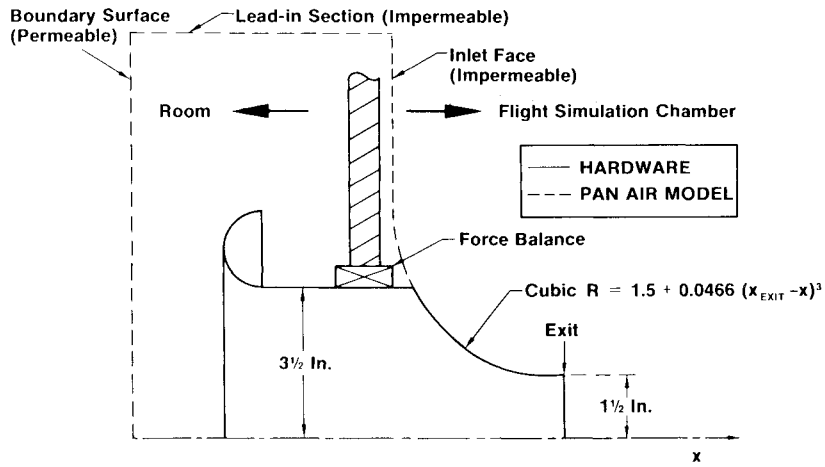

Fig. 2 3-in. exit diam cubic nozzle flowthrough installation in the FSC.

engine/airframe integration development.[9,10] The introduction of these more complete methods is changing the role of panel methods in configuration development. Nevertheless, PAN AIR's complete geometric generality and versatility will give it a continuing role in aero-propulsion integration.

Applications

The versatility of the PAN AIR system has led to its application to a variety of aero-propulsion problems. Examples of subsonic applications will be presented to illustrate some of the capabilities of the system. These include a study of the internal flow losses through a calibration nozzle, the calculation of surface pressures about an isolated nacelle, the modeling of exhaust flows, and the analysis of nacelle blowing (power) effects on a complete wing-body-strut-nacelle configuration.

Internal Flows

The flow about an aircraft propulsion system may be divided into an internal flow and an external flow. The internal flow encompasses the flow captured by the nacelle, including the upstream inlet streamtube and the downstream exhaust streamtube. In testing aircraft wind-tunnel models, the engine is frequently simulated by a simple flow-through system. In this type of testing, the force balance drag includes the internal flow drag, which can be on the order of 3 to 4% of the airplane drag in a typical underwing strut-mounted installation. In commercial airplane development it is desirable to know drag increments to within less than 1%. Internal skin friction estimates cannot reliably guarantee these accuracies. Instead, it has been the practice to determine the internal drags and to calibrate flow-through and powered nacelles through the use of a type of altitude test chamber called the Flight Simulation Chamber (FSC). In the FSC the inlet operates in an open room at ambient conditions while the flow exhausts into a tank at reduced static pressure. The flow nacelle is mounted on a force balance which measures the internal drag.

A study was begun whose long-term goal was to develop computational methods required for accurate calculation of the internal drag of an *installed* flow-through nacelle. In this way it was hoped that installation effects, such as suppression of the internal mass flow due to the airframe, could be determined. The first step of this study was to apply the coupled PAN AIR/boundary layer code to an isolated flow nacelle. A 3 in. diam "cubic" calibration nozzle previously tested in the FSC was selected to provide an experimental check on the computational results. The test configuration is illustrated in Fig. 2. The PAN AIR modeling used in the study is depicted in Fig. 3. Although it was possible to obtain an inviscid solution for the actual nozzle geometry, the presence of a corner at the beginning of the "cubic" section resulted in a boundary layer separation which, in turn, caused the boundary layer code to fail. Simple analysis indicated that losses in the constant area section would be very small due to the low velocities. The computational model was therefore simplified to provide a smooth entry into the nozzle and the boundary layer calculations were begun a short distance into the nozzle.

Composite source/doublet analysis networks were used to model inlet and nozzle. The entry section was represented by a boundary surface to permit mass flow entry and an impermeable lead-in section and inlet face. The exhaust was modeled by a near-field source/doublet wake and a far-field doublet wake. Note that there is no exit boundary surface.

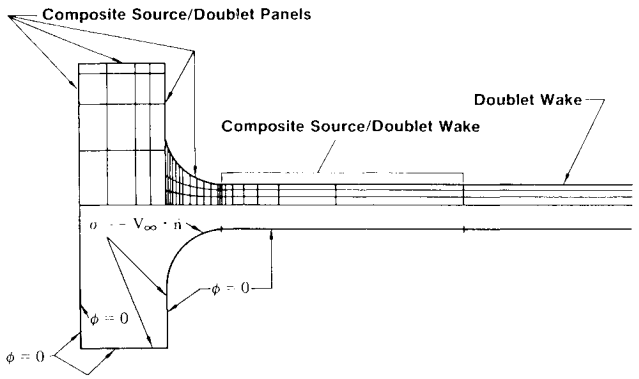

Fig. 3 PAN AIR modeling of 3 in. diam cubic nozzle static test installation.

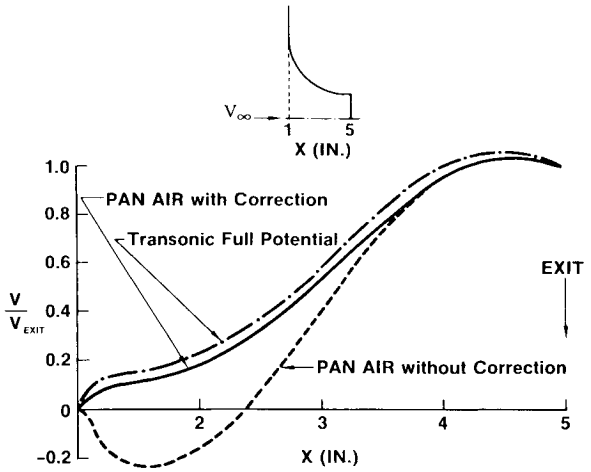

Fig. 4 Tangential velocity distribution on the 3 in. diam cubic nozzle wall.

The boundary conditions are shown in Fig. 3. Indirect mass flux boundary conditions[11] were used on all impermeable surfaces. The perturbation potential for the entire external surface was set to zero to insure that no external influence would affect the internal flow. The analysis was done at a freestream M equal to the exit M. A fully turbulent boundary layer was computed starting at about 10% of the cubic nozzle length with an initial momentum thickness specified. Sensitivity studies showed that valid solutions were not dependent on this initial momentum thickness. The boundary layer calculations were made for test values of Reynolds number and total temperature. Boundary layer momentum thickness and displacement thickness were computed at the nozzle exit using three iterations of the coupled PAN AIR/boundary layer code, thereby including the displacement effect of the boundary layer in the inviscid flow calculations.

Surface tangential velocity distributions along the "cubic" nozzle wall with and without a second order mass flux correction are shown in Fig. 4. It should be noted that, although the velocity distributions are radically different, they have been derived from the same solution based on mass flux impermeability. The mass flow vector is tangent to the surface, but in compressible flow the velocity vector is not. Because of the small perturbation assumptions implicit in the Prandtl-Glauert equation, significant errors are introduced into the compressible velocity computations when the local velocity deviates substantially from the freestream. The largest such deviations occur in and around stagnation regions such as at the wing leading edges and inside inlets. The following correction[5] is available within PAN AIR, in order

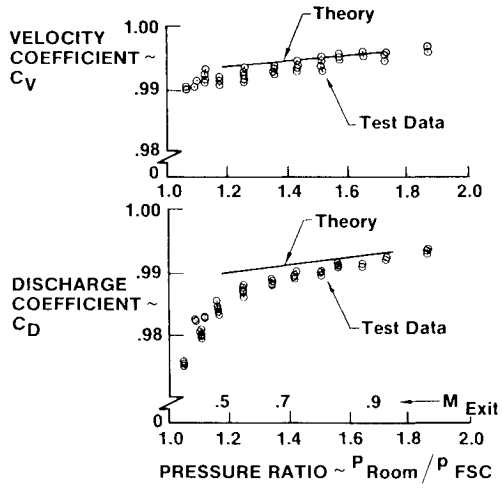

Fig. 5 Theoretical and experimental flow characteristics of a 3 in. diam calibration nozzle.

to make the velocity vector colinear with the mass flux vector.

$$\bar{V} = \frac{|\bar{V}|}{|\bar{W}|}\bar{W} \qquad \text{when } \phi_x > 0$$

$$= \frac{1}{1 - M_\infty^2 \phi_x / V_\infty}\bar{W} \qquad \text{when } \phi_x < 0$$

Figure 4 illustrates how significant the error in velocity can be for a stagnating flow if appropriate corrections are not made. Also shown are results from an axisymmetric full potential code.[12] The corrected PAN AIR results agree quite well with the full potential code results, which are not subject to the small disturbance assumption. The use of mass flux impermeability insures mass conservation through the duct. The subsequent use of the velocity correction improves the appearance of the solution and allows the velocities to be used as input in the boundary layer calculations.

For our thrust/drag bookkeeping procedures and for calibration in the FSC we define internal drag as the momentum difference of the internal flow at upstream and downstream infinities. The momentum at downstream infinity cannot be conveniently measured, but can be derived from measurements at the duct exit with the assumption of isentropic expansion to freestream static pressure. On this basis the internal drag equation can be written as:

$$\text{Internal Drag} = C_D \dot{m}_I V_\infty (1 - C_V)$$

where C_V is the velocity coefficient, the ratio of the velocities upstream to downstream infinity, and C_D is the discharge coefficient, the ratio of the actual mass flow through the nacelle to the ideal (inviscid) mass flow.

The velocity coefficient C_V and the discharge coefficient C_D of a flow nacelle can be determined from a static calibration of the nacelle in an altitude test chamber such as the FSC. These coefficients may also be determined from the boundary layer momentum thickness θ and displacement thickness δ^*.[11]

$$C_V = 1 - 4\frac{\theta_{EXIT}}{D_{EXIT}}$$

$$C_D = 1 - 4\frac{\delta^*_{EXIT}}{D_{EXIT}}$$

where D_{EXIT} is the nacelle exit diameter. Results obtained this way are shown in Fig. 5 with experimental data from the FSC.

Very good agreement in velocity coefficient was obtained. Although the agreement in the discharge coefficient is not quite as good, it is sufficient for accurate internal drag determination.

External Flow Around an Isolated Nacelle

PAN AIR can also be applied to the analysis of the external flow about nacelle configurations. The nacelles can be either flow-through or powered nacelles with specified inlet conditions. The modeling of a powered nacelle is illustrated in Fig. 6. Composite source/doublet analysis networks are used on all surfaces except for the wakes, which are doublet-wake networks. Indirect mass flux boundary conditions, also be used to simulate the boundary layer displacement effect via transpiration, are specified on all surfaces. An indirect mass flux boundary condition is also used on the inlet fan face to specify inlet mass flow. The exhaust flow modeling will be discussed in the following section.

Use of this computational model results in excellent agreement with experimental data on nacelles with attached subcritical flows. However, use of subcritical panel methods for isolated nacelle analysis has been superseded by more advanced methods such as those based on the Euler formulation.[14] This advanced method is capable of transonic flow analysis of isolated non-axisymmetric nacelles at angle of attack and includes a coupled 3-D boundary layer analysis. However, development of the Euler code, and the application of the 3-D boundary layer methods to nacelles were both aided by PAN AIR. Use of PAN AIR will continue for analyzing *installed* nacelles.

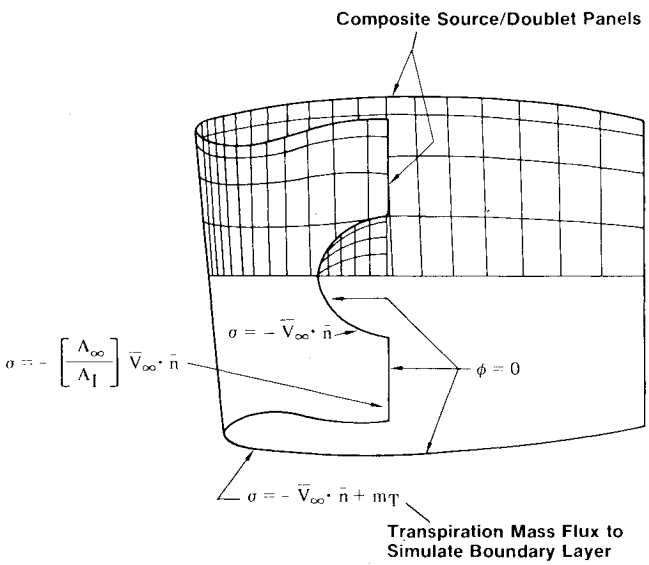

Fig. 6 Powered nacelle modeling.

Exhaust Jet Modeling

Exhaust jet calculations are not readily amenable to linear potential flow theory. The jets usually feature varying total pressures, mixed subsonic and supersonic regions with strong interactions with boundary layers, mixing layers and regions of separated flow. Such flows are more properly the subject of analysis using the Navier-Stokes equations. Unfortunately, it is not yet practical to use these more complete methods in the analysis of complex wing-body-nacelle configurations. It is therefore desirable to develope exhaust flow models which capture the essence of the real flow, yet are adaptable to analysis using the potential flow theory employed in panel methods and transonic finite volume calculations.

Three methods of modeling exhaust flows in potential flow are illustrated in Fig. 7. The first model is the most simple where the exhaust plume is modeled as a solid surface. The shape of the exhaust plume is usually derived from a more complete axisymmetric calculation such as Navier-Stokes, streamtube curvature, or a multi-stream transonic method. This model has been previously used successfully in panel methods,[2] and finite volume transonic analysis.[9] A disadvantage of this model is that the exhaust plume geometry must change to reflect such changes as exhaust fan nozzle pressure ratio, FNPR, or core-cowl geometry.

A variation of the solid plume model is shown in the second model. Here a solid plume shape is used to define the exhaust plume for the "ram" condition (exhaust at free stream velocity). At this condition the viscous effects are more benign and the flow is subcritical, making the calculation of the plume shape more reliable. Power effects are simulated by specifying a transpiration on the plume as a function of exhasut fan nozzle pressure ratio. The amount of transpiration is calibrated through comparison with a Navier-Stokes calculation or experimental data. This modeling has the advantage of requiring only one geometry, only one paneling in PAN AIR, and only one grid generation in a full potential or Euler equation finite volume analysis. An example of this type of exhaust flow modeling in a PAN AIR analysis will follow. The calibration of the transpiration on the plume with a Navier-Stokes solution will also be discussed.

A disadvantage of the first two exhast modeling methods is that the plume shape must still be defined. The third exhaust plume model illustrated in Fig. 7 overcomes this restriction. Here the exhaust plume is modeled as a wake instead of a hard surface. This requires that the geometry internal to the exhaust also be modeled. In a typical high-bypass-ratio

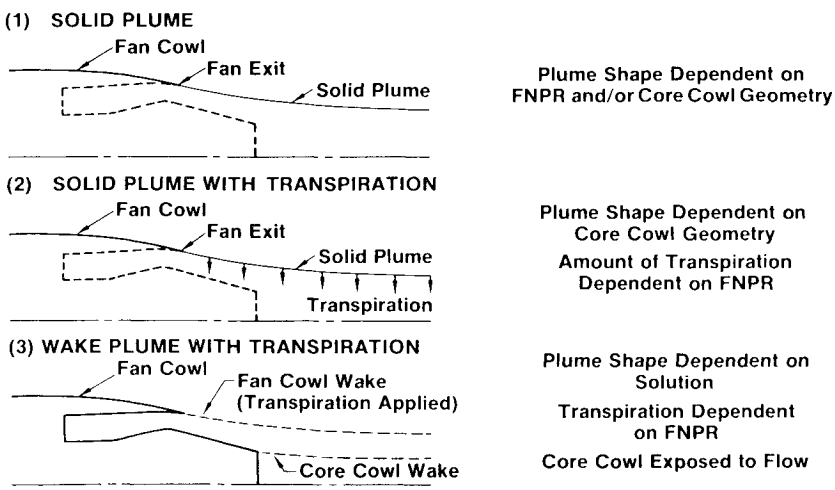

Fig. 7 Potential flow models for exhaust simulation.

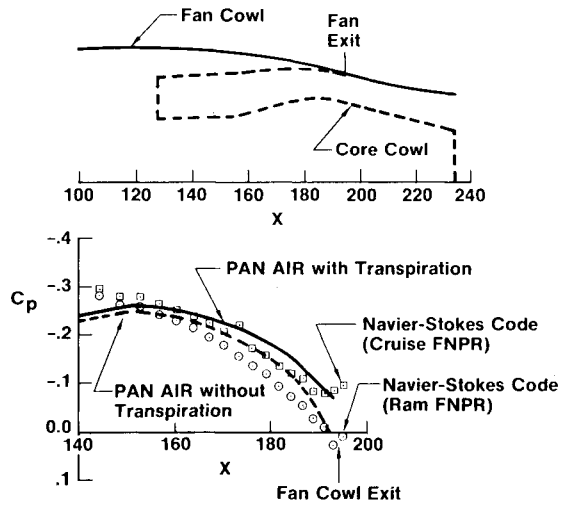

Fig. 8 Effect of transpiration on fan cowl pressures.

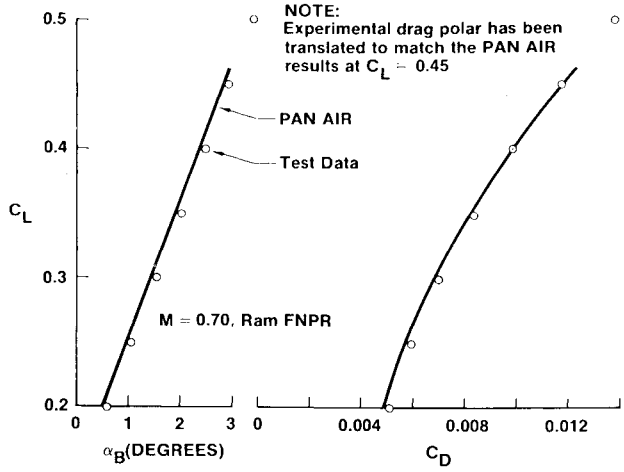

Fig. 10 Lift curve and drag polar of a transport airplane, $M_\infty = 0.70$, Ram FNPR.

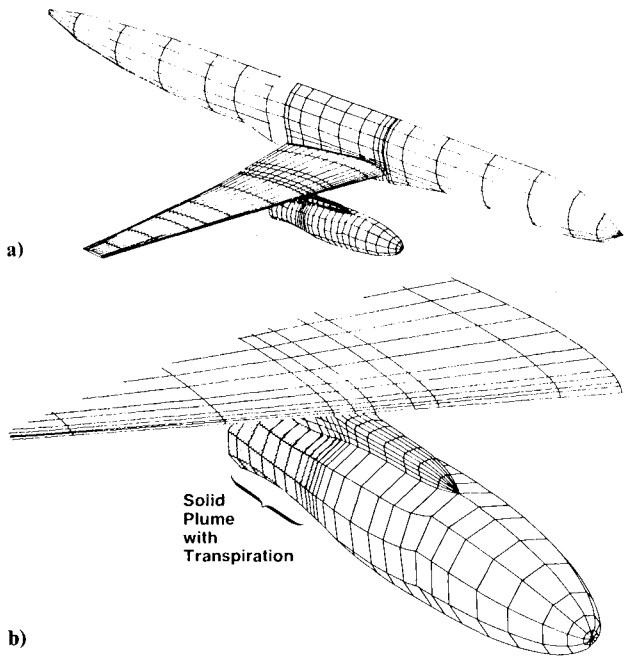

Fig. 9 Paneling for a wing-body, strut, blown-nacelle wind-tunnel model.

turbofan engine this would include the core cowl and a portion of the fan duct. Since the exhaust plume is modeled as a wake, its position is no longer critical to the solution. It is usually adequate to have the wake maintain a constant fan flow cross-sectional area. The plume surface is now permeable with only the specification of zero pressure jump across its surface. The flow is therefore free to react to the presence of the core cowl and the nearby strut and wing. Power effects may still be simulated through the use of transpiration by placing source panels on the wake surface.

The values of transpiration necessary to simulate various exhaust pressure ratios in the second and third models can be found by trial and error for an isolated case. Experimental data or results from a Navier-Stokes solution are used to calibrate the amount of transpiration. Figure 8 shows the pressure distributions obtained from PAN AIR and a Navier-Stokes[15] code on the fan cowl boattail of a modern high-bypass-ratio turbofan engine. Zero transpiration is used to simulate the "ram" condition, a negative value (i.e., a sink distribution) was found to simulate the "cruise" condition. Although the correlation between the inviscid linear PAN AIR solutions and the viscous non-linear Navier-Stokes solutions is only fair, the change in surface pressure on the fan cowl boattail as a function of fan nozzle pressure ratio is correctly simulated by the PAN AIR solutions. The absolute level of agreement was improved when a boundary layer solution for the fan cowl was included. While there might not be much value in using PAN AIR to simulate isolated powered nacelles for which there is already experimental data or more complete solutions, there is value in incorporating these calibrated PAN AIR models into an installed configuration. Alternatively, one can simulate exhaust effects by embedding an interactive Navier-Stokes solution within the PAN AIR system.[16]

Engine/Airframe Integration

The value of PAN AIR in engine/airframe integration lies in its ability to model complete wing-body-nacelle configurations. The inherent versatility of the geometry and boundary condition specifications allows PAN AIR to be used for analysis of complex configurations in its own right. Subcritical panel methods have been very successful in computationally determining the interference drag of current transport type configurations. References 2 and 3 illustrate the use of a first order panel method in determining the interference drag mechanisms of a wing strut-mounted nacelle and some of the concepts of designing low interference drag installations. In more recent times PAN AIR has been used to aid the development of finite volume transonic methods by providing solutions for direct comparison at subcritical conditions and by the development of new flow models such as the use of transpiration on the exhaust plume to simulate power effects.

A wind-tunnel half-model of a twin engine transport with blown nacelles was used during the development of the configuration to simulate exhaust effects. In this model high pressure air is routed past the force balance, through the wing and nacelle strut, and then exhausted out the aft end of the nacelle. The front end of the nacelle is domed to provide a streamline shape, but the aft end is identical to that of the actual engine. This type of model is typically used to determine the effects of engine exhaust on the airplane configuration. A PAN AIR paneling of this configuration is shown in Fig. 9. The entire configuration, including the plume and trailing wakes, was represented by 1292 panels. Indirect mass flux boundary conditions were specified for all solid surfaces. The exhaust is modeled using the second scheme of Fig. 7. The plume shape, which is included in the configuration paneling, was that for the "ram" fan nozzle pressure ratio obtained from a Navier-Stokes solution for the isolated nacelle. Cruise FNPR was simulated by applying the

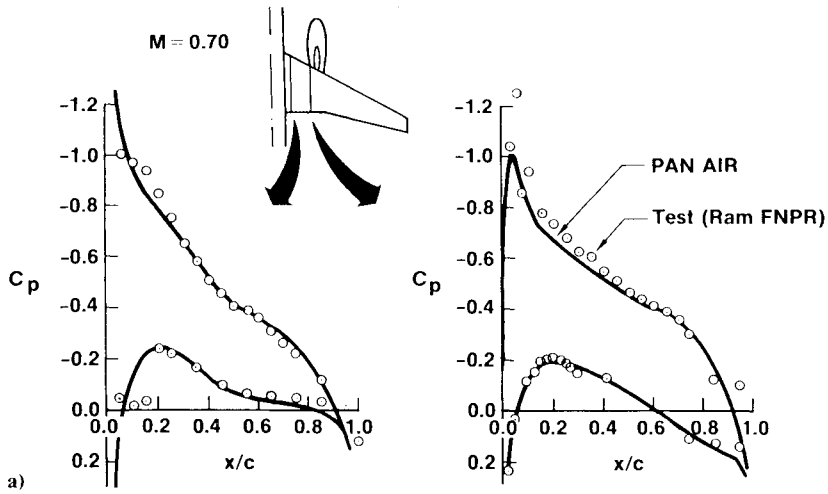

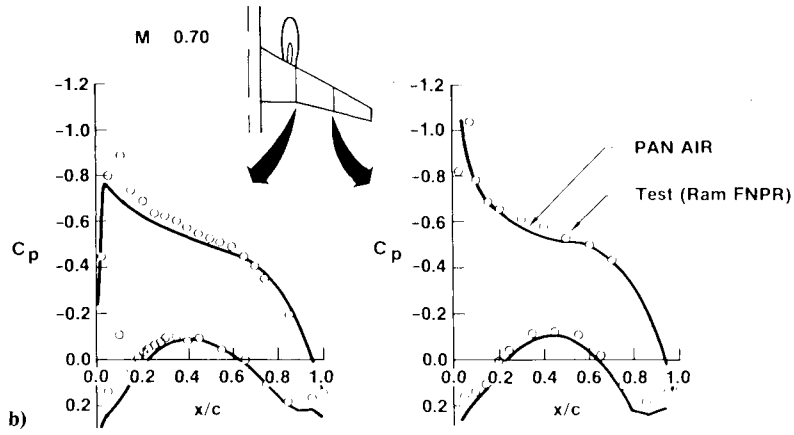

Fig. 11 Test/theory comparison for wing-body, strut, blown nacelle, $M_\infty = 0.70$.

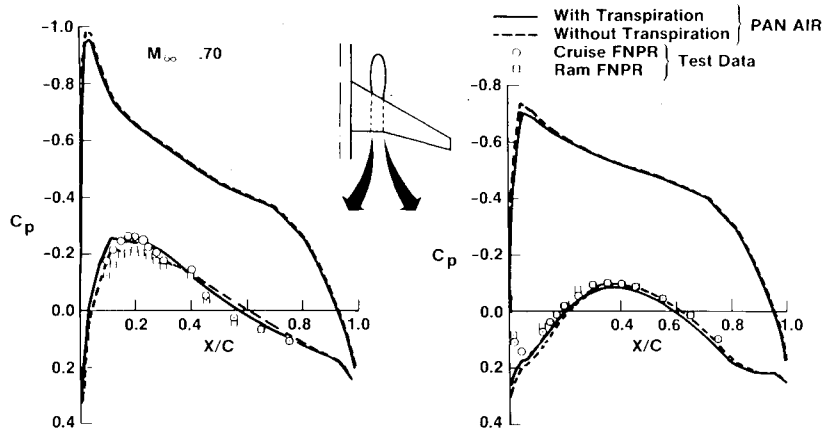

Fig. 12 Power effects on wing surface pressures.

transpiration determined in the isolated condition. PAN AIR solutions for both the "ram" and "cruise" pressure ratios were obtained within a single run for an essentially subcritical condition of M 0.70. No boundary layer calculations were made.

Lift and drag results from PAN AIR are shown with experimental data in Fig. 10. For the drag comparison the experimental drag polar has been translated to match the PAN AIR results at $C_L = 0.45$. The overall correlation is quite good. Figure 11 shows computed and experimental wing surface pressure distributions in a case where the nacelle exhausts at "ram" fan nozzle pressure ratio. Although good, the correlation could have been improved if the PAN AIR analysis were made at a slightly higher angle of attack. Figure 12 shows the computed and experimental wing pressures near the nacelle strut for both "cruise" and "ram" fan nozzle pressure ratios. PAN AIR correctly predicted the lower surface pressures and the effects of changing fan nozzle pressure ratio. Figure 13 shows the fan cowl surface pressures. Again the PAN AIR results show the proper trend of changing fan nozzle pressure ratio. The computational results suggest that most of the measured drag increase due to blowing (increased fan nozzle pressure ratio) appears on the inboard boattail of the fan cowl. A look at the force components from the integrated surface pressures revealed that the wing, the fuselage, and the nacelle strut all had favorable contributions, while the nacelle is the only component that contributed to a drag penalty. When the lost lift due to in-

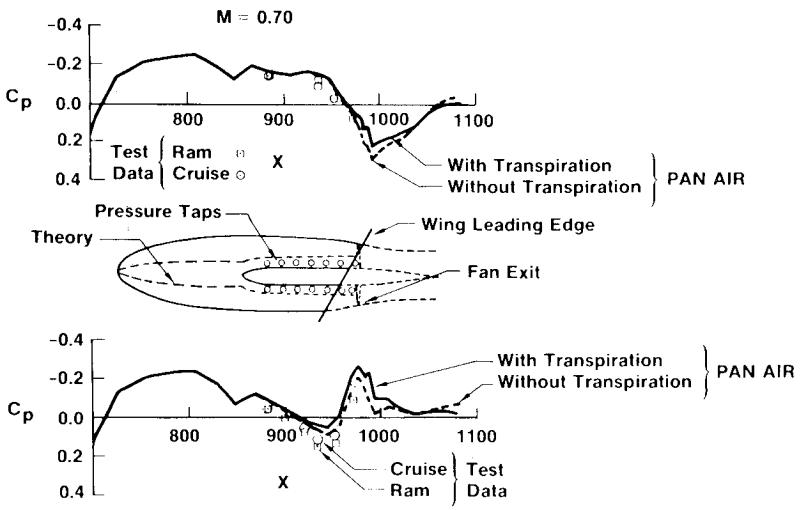

Fig. 13 Power effects on nacelle surface pressures.

creased blowing is restored and the induced drag associated with that is included, the computed blowing drag amounts to 1.3 drag counts. This compares with about 2 drag counts measured in the wind tunnel. While it is recognized that there may be other contributors to blowing drag, such as core cowl and viscous related effects not treated in this study, the PAN AIR results do seem to predict the correct trends and magnitudes for this subcritical case.

The computed blowing drag is based on integrated surface pressures from the PAN AIR solution. As long as there are no large changes in the paneling geometry (in this case only transpiration changed) the integrated pressure drags appear to be reliable with moderate panel densities. However, for major configuration change, such as nacelle-on/nacelle-off, integrated pressure drags may no longer be reliable without a substantial increase in panel density. For these cases, interference drags are usually based on induced drag calculations.

The exhaust flow model developed using PAN AIR for an isolated nacelle, and then validated for use in a complete wing-body-strut-nacelle has since been incorporated into a finite volume full potential transonic computational method.[10] This method allows analysis at higher Mach numbers where supercritical flows are present.

Conclusions

Several diverse applications of the PAN AIR system to aero-propulsion problems have been presented to demonstrate the versatility of the method. Panel methods have been used extensively in the recent development of several close-coupled nacelle installations. Panel methods, when used within their limits of applications, provide valuable insight into complex flow fields, guidance for achieving integrated designs, and an ability to explore innovative configuration designs. The proper coordination of computation and wind-tunnel testing can significantly reduce the time, risk, and expense of aero-propulsion integration development. The versatility of the PAN AIR system will give it a continuing role in the design and analysis of geometrically complex and/or innovative configurations. The emergence of non-linear transonic analysis methods has not led to the demise of panel methods, but, rather, has changed the mode in which they are used. For instance, PAN AIR has been used extensively as a standard of measure against which to check new geometric capabilities of transonic methods. Comparisons with a computational method of known validity lead to a far more accurate assessment of the transonic codes' numerical characteristics than would have been possible with comparisons of experimental data alone—data which tends to be clouded by measurement inaccuracies and viscous effects. Also, PAN AIR continues to be used on problems for which transonic methods do not yet provide sufficient geometric fidelity or modeling versatility.

Acknowledgement

This paper is based on work conducted for the Boeing Independent Research and Development Program. The authors would like to thank Mr. Frank L. Wright for the internal flow analysis presented in this paper.

References

[1]Henderson, W.C., and Patterson, J.C., Jr., "Propulsion Installation Characteristics for Turbofan Transports", AIAA-83-0087, Jan. 1983.

[2]Gillette, W.B., "Nacelle Installation Analysis for Subsonic Transport Aircraft", AIAA-77-102, Jan. 1977.

[3]daCosta, A.L., "Application of Computational Aerodynamics Methods to the Design and Analysis of Transport Aircraft", ICAS Paper No. 78.B2-01, Sept. 1978.

[4]Derbyshire, T., and Sidwell, K.W., "PAN AIR Summary Document", NASA CR-3250, (Version 1.0), April 1982.

[5]Magnus, A.E., and Epton, M.A., "PAN AIR - A Computer Program for Predicting Subsonic or Supersonic Linear Potential Flows About Arbitrary Configurations Using a Higher Order Panel Method", NASA CR-3251, Vol. 1, (Version 1.0), April 1980.

[6]Carmichael, R.L., and Erickson, L.L., "PAN AIR: A Higher Order Panel Method for Predicting Subsonic or Supersonic Linear Potential Flows About Arbitrary Configurations", AIAA-81-1255, June 1981.

[7]Moran, J., Tinoco, E.N., and Johnson, F.T., "User's Manual - Subsonic/Supersonic Advanced Panel Pilot Code," NASA CR-152047, Feb. 1978.

[8]Wigton, L.B., and Yoshihara, H., "Viscous-Inviscid Interactions with a Three-Dimensional Inverse Boundary Layer Code", Presented at Second Symposium on Numerical and Physical Aspects of Aerodynamic Flows, Jan. 17-20, 1983, California State University, Long Beach, Ca.

[9]Yu, N.J., "Transonic Flow Simulations For Complex Configurations With Surface-Fitted Grids," AIAA-81-1258, July 1981.

[10]Tinoco, E.N., and Chen, A.W., "Transonic CFD Applications to Engine/Airframe Integration," AIAA-84-0381, Jan. 1984.

[11]Morino, L., Chen, L.T., and Suciu, E.O., "Steady and Oscillatory Subsonic and Supersonic Aerodynamics Around Complex Configurations," AIAA Journal, Vol. 13, March 1975, pp. 368-375.

[12]Colehour, J.L., "Transonic Flow Analysis Using a Streamline Coordinate Transformation Procedure," AIAA-73-657, July 1973.

[13]Reimer, R.M., "Determination of ASME Nozzle Flow Coefficients by Thrust Measurement," ASME Paper No. 64-WA/FM-3, Nov. 1964.

[14]Chen, H.C., Yu, N.J., Rubbert, P.E., and Jameson, A., "Flow Simulations for General Nacelle Configurations Using Euler Equations," AIAA-83-0539, Jan. 1983.

[15]Peery, K.M., and Forester, C.K., "Numerical Simulation of Multi-Stream Nozzle Flows", AIAA-79-1549, July 1979.

[16]Roberts, D.W., "Prediction of Subsonic Aircraft Flows with Jet Exhaust Interactions", AGARD-CP-301, Paper No. 32, May 1981.